PROCEEDINGS OF SPIE

SPIEDigitalLibrary.org/conference-proceedings-of-spie

Application of the Fractional Fourier Transform for dispersion compensation in signals from a fiber-based Fabry-Perot interferometer

Marcin Mrotek
Jerzy Pluciński

SPIE.

Application of the Fractional Fourier Transform for dispersion compensation in signals from a fiber-based Fabry-Pérot interferometer

Marcin Mrotek[a] and Jerzy Pluciński[b]

[a,b]Politechnika Gdańska, ul. Narutowicza 11/12, Gdańsk, Poland

ABSTRACT

Optical methods of measurement do not require contact of a probe and the object under study, and thus have found use in a broad range of applications such as nondestructive testing (NDT), where noninvasive measurement is crucial. Measuring the refractive index of a material can give a valuable insight into its composition. Low-coherence radiation sources enable measurement of the sample's properties across a wide spectrum, while simultaneously measuring the absolute value of optical path difference between interfering waves, which is necessary to calculate the refractive index.

The measurement setup used in this study consists of a fiber-based Fabry-Pérot interferometer, illuminated by a low-coherence infrared source. The samples under measurement are located in the cavity of the interferometer, and their transmission spectra are recorded using an optical spectrum analyzer. Additional reference measurements are performed with the cavity filled with air, in order to precisely measure the geometrical length of the cavity.

The purpose of the study was to develop a digital signal processing algorithm to improve the resolution of analysis of the spectra of radiation measured at the output of the interferometer. This goal was achieved by decreasing the broadening of the signal in the Fourier domain caused by dispersion of the medium filling the cavity. The Fractional Fourier Transform is a generalization of the Fourier transform allowing arbitrary rotation of the signal in the time-frequency domain, allowing more precise analysis of signals with variable frequency. This property makes this transformation a valuable tool for the analysis of interferometric signals obtained from measurements of dispersive media, as the variable rate of change of the optical path length with respect to wavenumber in such media results in varying frequency of the modulation of measured spectra. The optical path difference inside the material under measurement is used together with the geometrical length obtained from the reference measurement in order to determine the refractive index. The parameters of the transformation are found by iterative adjustment to the signal under analysis.

The developed algorithm was tested using both real measured spectra and simulated signals based on a theoretical model of the interferometric setup, and its effectiveness was compared to previously used methods of analysis. It was found to increase the resolution of analysis up to the Fourier limit that occurs in signals with no dispersion.

Keywords: interferometry, Fabry-Pérot interferometer, optical fibers, Fractional Fourier Transform, time-frequency analysis

Further author information: (Send correspondence to Marcin Mrotek)
E-mail: marmrote@student.pg.gda.pl

Photonics Applications in Astronomy, Communications, Industry, and High Energy Physics Experiments 2017,
edited by Ryszard S. Romaniuk, Maciej Linczuk, Proc. of SPIE Vol. 10445, 1044511
 · doi: 10.1117/12.2281017

1. INTRODUCTION

Measurement of the refractive index of materials as a function of wavelength provides insight into their composition. Among the practical uses of refractive index measurements are hematocrit sensors and biological weapon detectors.[1–3] The real part of the complex refractive index of a material analysed in a cavity of a Fabry-Pérot interferometer can be obtained by locating the maxima of the Fourier transform of the measured spectrum.[4] One of the factors influencing the precision of this measurement is the width of the located peak of the transform, especially if the optical path length in the material inside the interferometer's cavity is short compared to the resolution of the spectral analyser used, or if signals from multiple interferometers with similar optical path lengths are connected in one optical fiber.

1.1 Measurement setup

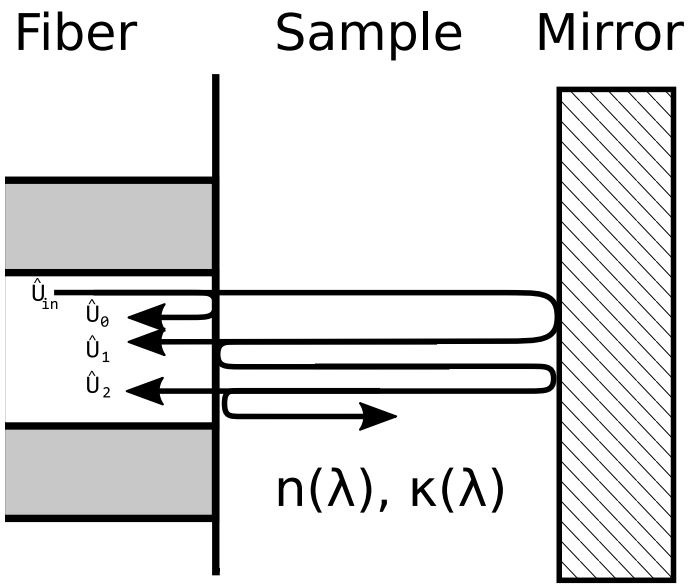

Figure 1. Measurement setup

The measurement setup, presented in fig. 1, consists of a fiber-based Fabry-Pérot interferometer, with a cavity formed between the ending of an optical fiber and a mirror. A single optical fiber is used to deliver the source radiation from a superluminescent diode, and to measure the output characteristic using an optical spectrum analysis.

2. THEORETICAL BASIS

2.1 Fractional Fourier Transform

The Fractional Fourier Transform is defined as an integral transformation (more specifically, a special case of the linear canonical transformation) of complex functions of a single variable[5]

$$f_a(u) \stackrel{\text{def}}{=} \int_{-\infty}^{\infty} K_a(u,t) f(t) dt, \tag{1}$$

where the kernel $K_a(u,t)$ is

$$K_a(u,t) = A_\alpha \exp\left(i\pi\left(\cot(\alpha)u^2 - 2\csc(\alpha)ut + \cot(\alpha)t^2\right)\right), \tag{2}$$

where $\alpha = \frac{a\pi}{2}$, and

$$A_\alpha = \sqrt{1 - i\cot\alpha}. \tag{3}$$

The square root in the above equation is defined such that the artument of the result lies in the interval $\left(-\frac{\pi}{2}, \frac{\pi}{2}\right]$.

2.2 Computation

The Fractional Fourier Transform can be more easily computed by relating it to the oridinary Fourier transforamtion. By combining equations (1), (2), and (3), and grouping the factors containing u^2, ut, and t^2 respectively, one can obtain

$$f_a(u) = A_\alpha \exp(\pi i \cot(\alpha) u^2) \int_{-\infty}^{\infty} \exp(-2\pi i \csc(\alpha) ut) \exp(\pi i \cot(\alpha) t^2) f(t) dt, \tag{4}$$

By substituting $u' = u \csc\alpha$

$$f_a(u') = A_\alpha \exp\left(\pi i \cot(\alpha) \frac{u'^2}{\csc^2\alpha}\right) \int_{-\infty}^{\infty} \exp(-2\pi i u' t) \exp(\pi i \cot(\alpha) t^2) f(t) dt, \tag{5}$$

one can obtain a form using the oridinary Fourier transform, denoted as $\mathfrak{F}\{\cdot\}$

$$f_a(u') = A_\alpha \exp\left(\pi i \cot(\alpha) \frac{u'^2}{\csc^2\alpha}\right) \mathfrak{F}\left\{\exp(\pi i \cot(\alpha) t^2) f(t)\right\}(u'). \tag{6}$$

Substituting back $u = \frac{u'}{\csc\alpha}$

$$f_a(u) = A_\alpha \exp\left(\pi i \cot(\alpha) u^2\right) \mathfrak{F}\left\{\exp(\pi i \cot(\alpha) t^2) f(t)\right\}(u \csc\alpha). \tag{7}$$

For $a = 1$ and thus $\alpha = \frac{\pi}{2}$ the above equation reduces to the oridinary Fourier transformation. Thus, the computation of the FrFT can be broken down into three steps:

- premultiplication with a t domain complex chirp,
- calculation of the oridinary Fourier transform,
- scaling in the u domain,
- postmultiplication with a u domain complex chirp,

A similar procedure can be used to efficiently compute the discrete FrFT using the Fast Fourier Transform algorithm.[6]

2.3 Fractional Fourier Transform of a Gaussian signal modulated with a chirp

Transfer functions of fiber-based Fabry-Pérot interferometers can be approximated (disregarding the Gouy phase shift) as infinite sums of sinusoids[7,8]

$$I_{\text{out}}(k) = I_{\text{in}}(k) \sum_{m=0}^{\infty} A_m \cos\left(\pi 2mnLk\right), \tag{8}$$

where I_{in} and I_{out} are the input and output signals respectively, A_m are the amplitudes (dimensionless, in relation to the intensity of the zero frequency component) of the components of the transfer function, n is the refractive index of the medium, L is the geometric length of the interferometer cavity, and k is the wavenumber. If the spectrum of the radiation source is Gaussian, the second component of the transfer function (for $m = 1$) will take the form of a Gaussian envelope modulated with a sinusoid. If the refractive index varies with the wavenumber but the range of variation is small in the analyzed part of the spectrum centered around a chosen wavenumber k_0, it can be approximated with the Taylor expansion $n(k_0 + \Delta k) \approx n(k_0) + \frac{dn(k_0)}{dk}\Delta k$. The phase term can then be approximated by

$$2\pi n(k)Lk \approx 2\pi Ln(k_0)k_0 + 2\pi L\left(n(k_0) + \frac{dn(k_0)}{dk}k_0\right)\Delta k + 2\pi L\frac{dn(k_0)}{dk}\Delta k^2 \tag{9}$$

In that case, the second component of the output signal is a linear chirp with a Gaussian envelope

$$x(k_0 + \Delta k) = \exp\left(-\frac{1}{2}\left(\frac{k_0 + \Delta k}{\sigma}\right)^2\right)\cos\left(2\pi Ln(k_0)k_0 + 2\pi L\left(n(k_0) + \frac{dn(k_0)}{dk}k_0\right)\Delta k + 2\pi L\frac{dn(k_0)}{dk}\Delta k^2\right), \tag{10}$$

where σ is the width of the Gaussian envelope. As the first step of calculating the Fractional Fourier Transform is a multiplication with a linear chirp

$$x'(k) = x(k)\exp\left(\pi i\cot(\alpha)\left(\frac{\Delta k}{\Delta k_s}\right)^2\right), \tag{11}$$

where Δk_s is the sample rate, the positive frequency component of the signal from eq. (10) after the multiplication becomes

$$x'(k) = \exp\left(-\frac{1}{2}\left(\frac{k_0 + \Delta k}{\sigma}\right)^2\right)\cdot \tag{12}$$

$$\cdot\exp\left(i2\pi Ln(k_0)k_0 + i2\pi L\left(n(k_0) + \frac{dn(k_0)}{dk}k_0\right)\Delta k + i\left(\pi\frac{\cot(\alpha)}{\Delta k_s^2} + 2\pi L\frac{dn(k_0)}{dk}\right)\Delta k^2\right). \tag{13}$$

For the α parameter such that

$$\cot\alpha = -2L\frac{dn(k_0)}{dk}\Delta k_s^2 \tag{14}$$

the chirp disappears and the function is reduced to a complex Gaussian impulse modulated by constant frequency $2\pi L\left(n(k_0) + \frac{\delta n(k_0)}{\delta k}k_0\right)$. Thus it can be seen that the broadening of the spectrum due to the chirp present in the signal can be mitigated by the appropriate choice of α. Moreover, finding the appropriate α determines the value of $\frac{\delta n(k_0)}{\delta k}$, which can be used to calculate the $n(k_0)$ from the frequency of the modulation of the spectrum, and possibly also provide further insight into the material's composition on its own.

3. NUMERIC ALGORITHM

In order to find the value of α that nullfies the chirp rate of the signal under analysis, it is enough to find the local maximum of the signal's Fractional Fourier Transform, similarly to results obtained for the chirplet transformation as detailed in.[4] As the analysed signal is given as a sequence of samples, the elaborated algorithm locates the maximum of the discrete-time analog of the fractional Fourier transform of the signal.

$$f(\alpha, u) = \sum_{n=0}^{N} x_n \sqrt{1 - i\cot\alpha} \exp\left(i\pi\left(\cot(\alpha)u^2 - 2\csc(\alpha)un + \cot(\alpha)n^2\right)\right), \tag{15}$$

The maximum of the transform is located by using the gradient descent method. The gradient of $f_a(u)$ with respect to α and u was computed with the forward-mode automatic differentiation algorithm. This method takes advantage of dual numbers defined as $(a + b\epsilon)$, where a and b are real numbers, while $\epsilon \neq 0$ and $\epsilon^2 = 0$. The algebraic properties of the dual numbers, together with the definitions of trigonometric functions of a dual variable

$$\begin{aligned}
\cos(a + \epsilon b) &= \cos a - \epsilon b \sin a, \\
\sin(a + \epsilon b) &= \sin a + \epsilon b \cos a, \\
\cot(a + \epsilon b) &= \cot a - \epsilon b \csc^2 a, \\
\csc(a + \epsilon b) &= \csc a - \epsilon b \csc a \cot a,
\end{aligned} \tag{16}$$

allow computation of the derivatives of any function composed of elementary functions by evaluating it for a dual argument:

$$\begin{cases} f(\alpha + \epsilon, u) = f(\alpha, u) + \epsilon \frac{\delta f(\alpha,u)}{\delta \alpha} \\ f(\alpha, u + \epsilon) = f(\alpha, u) + \epsilon \frac{\delta f(\alpha,u)}{\delta u} \end{cases} . \tag{17}$$

As the gradient descent algorithm can converge on any local maximum near the starting point, this point must be chosen carefully. It was determined that using the local maximum of the regular Fourier Transform of the signal corresponding to the chosen frequency component is an adequate starting point.

4. RESULTS

The elaborated algorithm was used to analyze signals obtained by mesuring the output spectra of the interferometer with a cavity filled with water, with geometric lengths of 150 µm and 200 µm, and using a superluminescent diode with a central wavelength of 1310 nm. Each measurement was paired with a reference measurement, which was performed with the same geometric length of the interferometer cavity which was filled with air.

In accordance with expectations, the results show that the sample measurements consistently show the presence of dispersion, while the reference measurement do not. In order to analyse the resulting data, initially the peak of the regular Fourier Transform corresponding to the lowest frequency of modulation was located. Two analyses were performed in order to measure the effect of using the FRFT: measuring the value of the transform in function of α across a chosen range, and locating points at half this value, in order to measure the FWHM of the peak of the transform.

The analysis results are presented in table 1. As the considered values of α are close to $\frac{\pi}{2}$ (i.e. the FRFT is close to the regular Fourier transformation), $\Delta\alpha$ in the table and the figures is defined in relation to the α parameter of the FRFT as

$$\Delta\alpha = \alpha - \frac{\pi}{2}. \tag{18}$$

As it seen from the results and figures 2 and 4 , the value of $\Delta\alpha$ at the maximum of the FRFT of the signal depends on the chromatic dispersion of the material of the sample, and on the geometric length of the sample.

Table 1. Results of the analysis

geometric length [µm]	material	chromatic dispersion[9,10] [µm^{-1}]	$\Delta\alpha$ of maximum	FWHM reduction
150	air	-0.0000013774	$-3.33 \cdot 10^{-8}$	0.0%
150	water	-0.015000	$-9.393 \cdot 10^{-8}$	0.5%
200	air	-0.0000013774	$-3.393 \cdot 10^{-8}$	0.0%
200	water	-0.015000	$-1.06 \cdot 10^{-7}$	0.5%

In every case, it was found that using the FRFT leads to a reduction in the FWHM of the signal's transform, as shown in figures 3 and 5. In the fig. 6 a comparison of analyses of both water samples is shown.

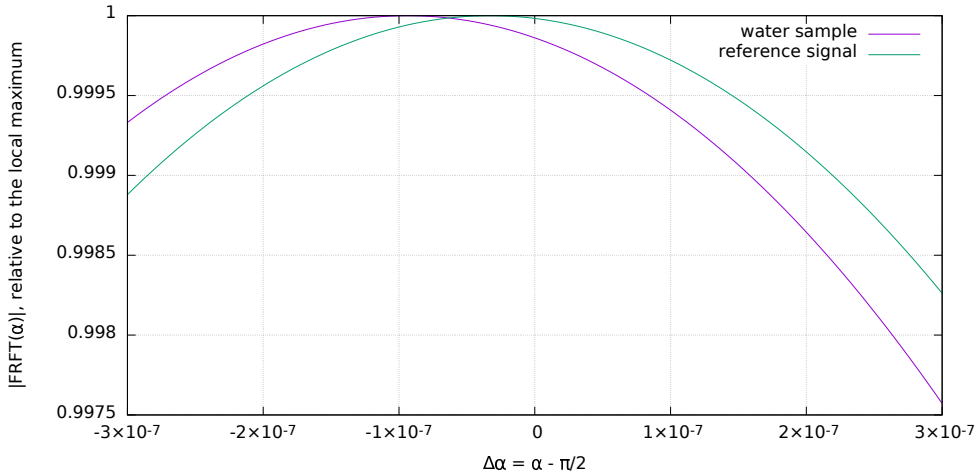

Figure 2. Comparison of the absolute value of the maximum of the Fractional Fourier Transforms of signals obtained from 150 µm water sample measurement and a reference measurement (with the interferometer cavity filled with air). The reference signal's maximum is located at $\alpha = 0$, while the sample signal's maximum is shifted due to dispersion.

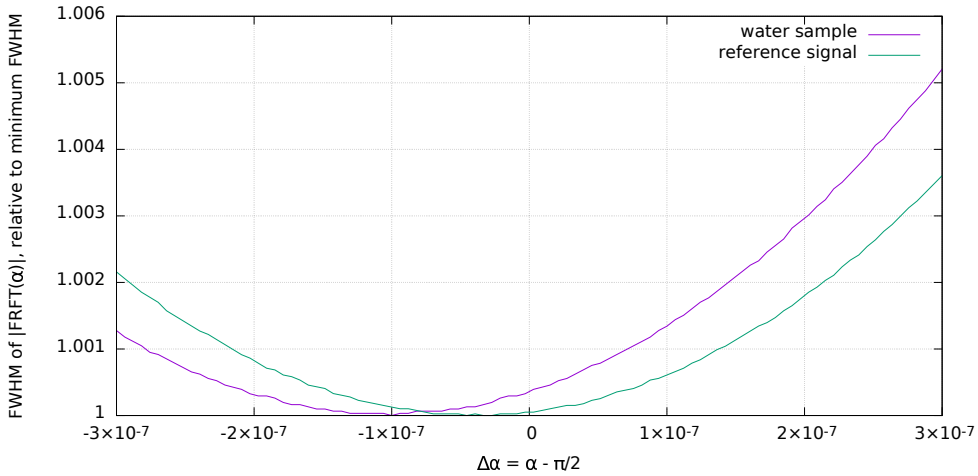

Figure 3. Comparison of the mimimum width of the Fractional Fourier Transforms of signals obtained from 150 µm water sample measurement and a reference measurement (with the interferometer cavity filled with air). The reference signal's minimum width is located at $\alpha = 0$, while the sample signal's minimum width is shifted due to dispersion.

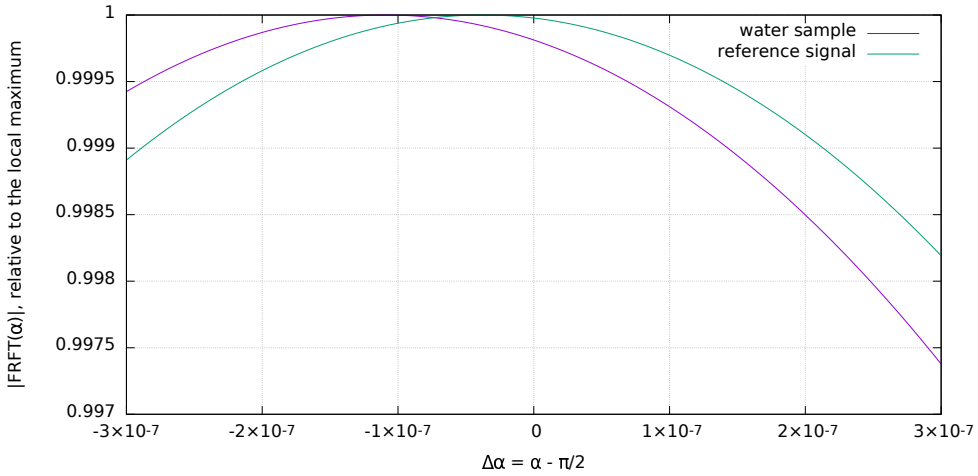

Figure 4. Comparison of the absolute value of the maximum of the Fractional Fourier Transforms of signals obtained from 200 µm water sample measurement and a reference measurement (with the interferometer cavity filled with air). The reference signal's maximum is located at $\alpha = 0$, while the sample signal's maximum is shifted due to dispersion.

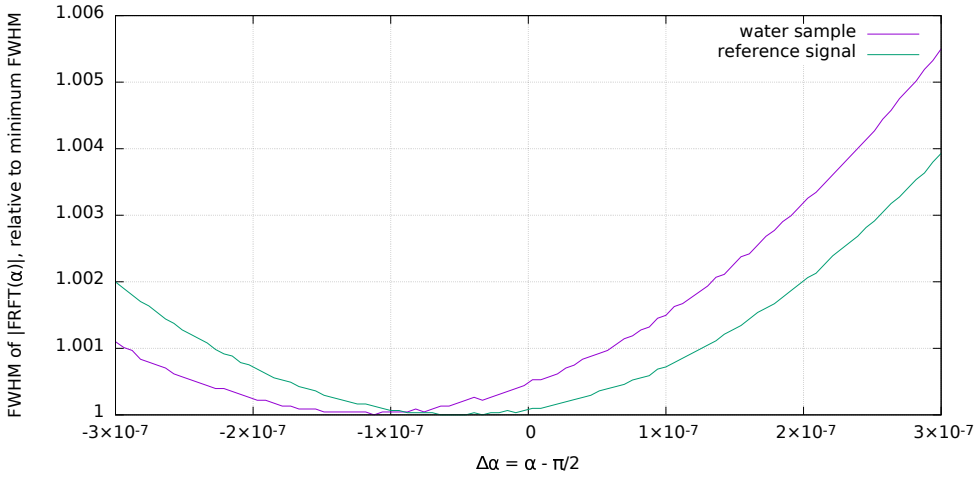

Figure 5. Comparison of the mimimum width of the Fractional Fourier Transforms of signals obtained from 200 µm water sample measurement and a reference measurement (with the interferometer cavity filled with air). The reference signal's minimum width is located at $\alpha = 0$, while the sample signal's minimum width is shifted due to dispersion.

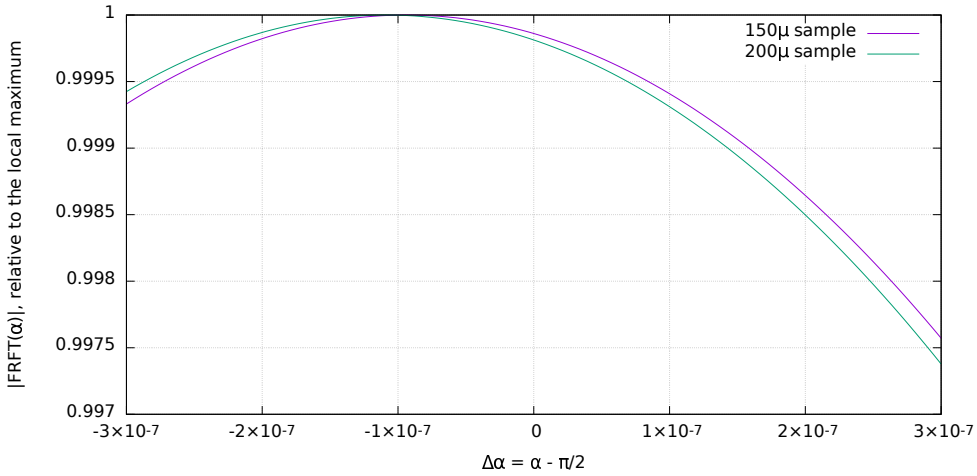

Figure 6. Comparison of the absolute value of the maximum of the Fractional Fourier Transforms of signals obtained from 150 µm and 200 µm water samples measurements.

5. CONCLUSION

The elaborated algorithm provides a means of detecting dispersion in measured spectrograms, compensating the widening of the spectrum and shift of the modulation frequency that is caused by it.

While the decrease of the width of the peaks in the Fourier transform is small, the α parameter of the transform's maximum, corresponding to the difference between the fractional Fourier transformation and the regular Fourier transformation, was found to be dependent on the chromatic dispersion and geometric length of the samples.

It is conjectured that using a radiation source with wider spectrum, samples with longer geometric lengths, and a spectral analyser with a higher resolution, could lead to more pronounced decrease in the width of the peaks. Moreover, the results obtained during the research show possibility of measuring the dispersion of analysed materials using the developed method. Further study is required to investigate the feasibility of these proposals.

REFERENCES

[1] Wierzba, P., Jędrzejewska-Szczerska, M., *Optimization of a Fabry-Perot Sensing Interferometer Design for an Optical Fiber Sensor of Hematocrit Level*, Acta Physica Polonica A, 124 (3), 586-588 (2013).

[2] Milewska, D., Karpienko, K., Jędrzejewska-Szczerska, M., *Application of thin diamond films in low-coherence fiber-optic Fabry-Pérot displacement sensor*, Diamond and Related Materials, vol.64, 169-176 (2016).

[3] Majchrowicz, D., Hirsch, M., Wierzba, P., Bechelany, M., Viter, R., Jędrzejewska-Szczerska, M., *Application of Thin ZnO ALD Layers in Fiber-Optic Fabry-Pérot Sensing Interferometers* SENSORS, vol.16, 416 (2016).

[4] Mrotek, M., *Analiza sygnału pomiarowego z interferometru niskokoherencyjnego*, master's thesis (2016).

[5] Ozaktas, H. M., Zalevsky, Z., Kutay, M. A., *The Fractional Fourier Transform with Applications in Optica and Signal Processing*, Wiley Series in Pure and Applied Optics (2001).

[6] Ozaktas, H. M., Arikan, O., Kutay, M. A., Bozdagi, G., *Digital Computation of the Fractional Fourier Transform*, IEEE TRANSACTIONS ON SIGNAL PROCESSING, VOL. 44, NO. 9 (SEPTEMBER 1996).

[7] Pluciński, J., Karpienko, K., *Fiber optic Fabry-Pérot sensors: modeling versus measurements results*, Proc. SPIE 10034, 11th Conference on Integrated Optics: Sensors, Sensing Structures, and Methods, 100340H (September 2, 2016).

[8] Pluciński, J., Karpienko, K., *Response of a fiber-optic Fabry-Pérot interferometer to refractive index and absorption changes: modeling and experiments*, Proc. SPIE 10161, 14th International Conference on Optical and Electronic Sensors, 101610F (10 November 2016).

[9] Ciddor, P. E., *Refractive index of air: new equations for the visible and near infrared*, Appl. Optics 35, 1566-1573 (1996).

[10] Hale, G. M., Querry, M. R., *Optical constants of water in the 200-nm to 200-μm wavelength region*, Appl. Opt. 12, 555-563 (1973).